LBL-14270

CONF-820927--9

Lawrence Berkeley Laboratory

UNIVERSITY OF CALIFORNIA

EARTH SCIENCES DIVISION

Presented at the 57th Annual Fall Conference of the Society of Petroleum Engineers, New Orleans, LA, September 26-29, 1982

NONISOTHERMAL EFFECTS DURING INJECTION AND FALLOFF TESTS

S.M. Benson and G.S. Bodvarsson

September 1982

NOTICE
PORTIONS OF THIS REPORT ARE ILLEGIBLE.
It has been reproduced from the best available copy to permit the broadest possible availability.

Prepared for the U.S. Department of Energy under Contract DE-AC03-76SF00098

DISTRIBUTION OF THIS DOCUMENT IS UNLIMITED

DISCLAIMER

This report was prepared as an account of work sponsored by an agency of the United States Government. Neither the United States Government nor any agency Thereof, nor any of their employees, makes any warranty, express or implied, or assumes any legal liability or responsibility for the accuracy, completeness, or usefulness of any information, apparatus, product, or process disclosed, or represents that its use would not infringe privately owned rights. Reference herein to any specific commercial product, process, or service by trade name, trademark, manufacturer, or otherwise does not necessarily constitute or imply its endorsement, recommendation, or favoring by the United States Government or any agency thereof. The views and opinions of authors expressed herein do not necessarily state or reflect those of the United States Government or any agency thereof.

DISCLAIMER

Portions of this document may be illegible in electronic image products. Images are produced from the best available original document.

LBL--14270

DE84 012250

NONISOTHERMAL EFFECTS DURING INJECTION AND FALLOFF TESTS

S. M. Benson and G. S. Bodvarsson

Earth Sciences Division
Lawrence Berkeley Laboratory
University of California
Berkeley, California 94720

DISCLAIMER

This report was prepared as an account of work sponsored by an agency of the United States Government. Neither the United States Government nor any agency thereof, nor any of their employees, makes any warranty, express or implied, or assumes any legal liability or responsibility for the accuracy, completeness, or usefulness of any information, apparatus, product, or process disclosed, or represents that its use would not infringe privately owned rights. Reference herein to any specific commercial product, process, or service by trade name, trademark, manufacturer, or otherwise does not necessarily constitute or imply its endorsement, recommendation, or favoring by the United States Government or any agency thereof. The views and opinions of authors expressed herein do not necessarily state or reflect those of the United States Government or any agency thereof.

This work was supported by the Assistant Secretary for Conservation and Renewable Energy, Office of Renewable Technology, Division of Geothermal and Hydropower Technologies of the U. S. Department of Energy under Contract No. DE-AC03-76SF00098.

DISTRIBUTION OF THIS DOCUMENT IS UNLIMITED

ABSTRACT

Injection tests are commonly performed in geothermal wells to obtain reservoir and well parameter data. Most of the tests are analyzed assuming that either the injected fluid is the same temperature as the reservoir fluid or that a stationary boundary separates the reservoir regions of different fluid properties. In general, neither of these assumptions are appropriate for the analysis of nonisothermal injection tests. Pressure transients in response to nonisothermal injection are controlled, to a great extent by the temperature-dependent fluid properties, viscosity and density. In this study, numerically simulated pressure transients during injection and falloff tests are analyzed to develop methods for obtaining the correct permeability-thickness of the reservoir and the skin factor for the well.

The results show that to correctly analyze pressure transients governed by a moving thermal front, the values used for the fluid properties must correspond to the temperature of the injected fluid. On the other hand, for pressure falloff tests and for injection tests conducted in a well cooled by previous injection or drilling, the physical properties of the in situ reservoir fluids must be used. It is also shown that the application of conventional isothermal methods for calculating skin values from injection and falloff data will give erroneous results. A new method is presented for calculating skin values from injection and falloff data that accurately corrects for nonisothermal effects. A number of detailed examples are given that illustrate the suggested method of analysis. The technique is applied to the analysis of injection test data from a well located in the East Mesa geothermal field in southern California.

INTRODUCTION

Injection tests in geothermal wells are commonly performed for three specific purposes: (1) to obtain pressure transient data from which the reservoir transmissivity and skin factor of the well can be calculated, (2) to stimulate naturally fractured geothermal wells, and (3) to determine the cause of reinjection problems. Usually, the temperature of the injected fluid is different from that of the in situ reservoir fluid. In order to interpret the pressure transient data correctly from any of these tests, the effect of nonisothermal reservoir conditions must be understood. For the interpretation of well test data, the two most important temperature-dependent properties of water are the dynamic viscosity and density. In Figure 1, the dynamic viscosity and density of water are plotted as a function of temperature. Between 20°C and 300°C the viscosity changes by an order of magnitude: the major change occuring between 20°C and 100°C. The fluid density decreases by approximately 30% between 20°C and 300°C.

During nonisothermal injection, a radial thermal-discontinuity is formed around the well. With increased injection, the distance to the discontinuity increases. Both the effect of this radial discontinuity and the effects of the moving thermal front on the pressure transient response must be considered to correctly interpret nonisothermal injection and falloff tests.

Numerous studies have been published on the analysis of well test data in reservoirs with radial discontinuities. Many of these have dealt with discontinuities created by waterflooding, steam injection or in situ combustion. One of the earliest papers, authored by Hazebroek et al.[1], presented a method for analyzing pressure falloff tests in water injection wells. The

method is based on a trial and error procedure in which the late time pressure transient data are adjusted to make them linear on a pressure vs. log (time) plot. Using this procedure, the correct average reservoir pressure, the permeability-thickness of the reservoir and the skin factor of the the well can be determined. Several other authors have reported on the development of analytic solutions or approximate analytic solutions for calculating pressure transients in composite reservoir systems with a stationary boundary separating the reservoir regions of different fluid or rock properties[2-6]. These studies show that two semi-log straight lines should be observed, the first corresponding to the rock or fluid properties of the inner region, and the second one to the properties of the outer region. The permeability-thickness of the two reservoir regions can be calculated from the slopes of the two semi-log straight lines. The skin factor for the well can be calculated with conventional methods from the first semi-log straight line. The radial distance to the discontinuity can be evaluated from the time at which the two semi-log straight lines intersect. Numerical methods have also been used to simulate the pressure falloff in systems with radial discontinuities[7-9]. These authors have investigated the effects of different mobility ratios, storage capacity ratios, afterflow, and the presence of reservoir boundaries on the pressure transient data. They show that unless the storage capacity is nearly the same on both sides of the discontinuity, the slope of the second semi-log straight line can not be used to calculate the permeability-thickness of the outer region. Furthermore, if the afterflow is large, it may not be possible to determine the properties of the inner region and the calculated distance to the discontinuity is erroneous. In these papers, guidelines are given to avoid misinterpretation of falloff data affected by these problems.

Satman et al.[10] compared and summarized some of the studies on pressure transients in systems with radial discontinuities.

More recently, several papers have been published that discuss the interpretation of pressure buildup and falloff tests in geothermal injection wells. Bodvarsson and Tsang[11] used a numerical simulator to study the pressure transient response during cold water injection into a hot water reservoir. They illustrated the effects of the temperature dependent fluid properties (viscosity and density) and the influence of a moving thermal boundary on the pressure response. Tsang and Tsang[12] developed a semi-analytic solution for calculating the pressure buildup during nonisothermal injection. This work verified the results of previous numerical studies and provided an approximate semi-analytic method for predicting the pressure behavior in an idealized well/reservoir system. O'Sullivan and Pruess[13] and Garg and Pritchett[14] studied the problem of cold water injection into a two-phase geothermal reservoir. All of the above studies demonstrate that the permeability-thickness of the reservoir can be calculated from pressure build-up data by using conventional analysis methods. Methods for calculating the skin factor of the well during non-isothermal tests have not been presented.

In the present study, analysis methods for evaluating the permeability-thickness of the reservoir and the skin factor of the well are developed. Several non-ideal factors are considered, including the effects of a diffuse and moving thermal front, that of a pre-existing cold spot around the wells and wellbore storage.

APPROACH

For the purpose of this study, a numerical simulator was used to generate pressure transient data during nonisothermal injection and fall-off tests. Simulations of both hot water injection into a cold reservoir and cold water injection into a hot reservoir were performed. However, because of the practical importance of the case of cold water injection into a hot reservoir (geothermal reinjection), the examples cited in this paper are limited to this case. The results are just as applicable to the inverse problem, that is, hot water injection into a cold reservoir.

The description of the reservoir/well model used in this study is as follows:

1) The reservoir is of uniform and constant porosity, compressibility, permeability, heat capacity, and thermal conductivity.

2) The reservoir is horizontal, infinite, of constant thickness, and bounded above and below by impermeable rock.

3) Thermal conduction to the cap rock and bedrock is neglected.

4) The reservoir is completely filled with slightly compressible liquid water.

5) Gravity slumping of the cold water front is neglected.

6) The well has a finite radius and fully penetrates the reservoir.

7) The intrinsic permeability of the formation is independent of temperature.

Several of the constraints on the present study warrant discussion. First, during nonisothermal injection it is well known that the density contrast between the fluids creates a tilting of the thermal front. The degree of tilting depends on a number of factors including the vertical permeability of the rock and the duration of injection. As many porous

medium formations consist of interbedded sands and shales, the vertical permeability is lower than the horizontal permeability. This tends to inhibit tilting of the front. Also, since the present study is concerned primarily with injection testing when the thermal front has not advanced very far away from the well, the importance of front tilting is minimal. A second constraint in this work is that the absolute permeability of the rock is independent of the temperature. There are studies which suggest that the rock permeability might be temperature sensitive[15,16]. However, because in the problem considered here the thermal front remains relatively close to the well, temperature dependent rock properties should be reflected by changes in the skin factor of the well, rather than the overall permeability of the system. Changes in the skin factor can be evaluated using the methodology presented in this paper. Therefore, this latter constraint does not limit the generality of the approach presented here.

Numerical Model

The numerical simulator PT (pressure-temperature) was used to simulate the nonisothermal injection and falloff tests. The simulator is three-dimensional and solves the mass and energy transport equations for a liquid-saturated, heterogeneous, porous and/or fractured medium. It employs the "integrated finite difference method" for discretizing the medium and formulating the governing equations[17]. The set of linear equations is solved at each timestep by direct means using an efficient sparse matrix solver.[18]

The simulator is quite general, as it allows for temperature- and/or pressure-dependent fluid and rock properties. The fluid density is calculated

as a function of pressure and temperature, using a polynomial approximation that is accurate to within 1%. Fluid viscosity is calculated as a function of temperature using an accurate (within 1%) exponential expression. The simulator has been validated against many analytical solutions as well as field experiments.[19] A detailed description of the simulator is given by Bodvarsson.[20]

Grid Size and Time Steps

A single-layer 1-m thick radial mesh (concentric circles) with a realistic wellbore radius of 0.1 m was used in the study. Close to the well very fine elements (10 X 0.1m, 8 X 0.2 m and 5 X 1 m) were used for accurate modeling of temperature variations during injection and falloff. Farther away from the well, the mesh spacing increases logarithmically for accurate modeling of the pressure response. A total of 86 elements were used. The outer boundary of the mesh, at 20,000 m from the axis of the system, is sufficiently distant so that boundary effects do not influence the calculations.

The time steps are automatically selected by the numerical code, based upon user-specified criteria for the maximum allowable pressure and temperature changes during each time step. For most runs a maximum allowable pressure and temperature change of 1 bar and 1°C were specified. We conducted a sensitivity study of the effects of grid size and time steps on the results and found that the results were practicaly independent of the grid size and time steps selected.

PRESSURE TRANSIENT BEHAVIOR DURING NONISOTHERMAL INJECTION

To illustrate the pressure transient behavior during nonisothermal (cold water) injection, a graph of the simulated pressure vs. log (t/r_D^2) is shown in Figure 2. The temperatures of the injected and reservoir fluids are 95°C and 250°C, respectively. At early times, the pressure transients are identical to those for 250°C isothermal injection (see 250°C this line in Figure 2). After a period of time, the slope of the semilog straight line changes and becomes identical to that for isothermal 95°C injection (see 95°C This line in Figure 2). Note that the pressure transients at several radii are plotted. All of the data points fall on the same curve when plotted in terms of (t/r_D^2). The temperature data at several distances from the injection well are also plotted in the top of Figure 2. Note that in each case, the change in slope of the semi-log straight line occurs when the thermal front passes.

The relationship between the change of slope on the semilog plot and the movement of the thermal front can be derived as follows. Assuming piston-like displacement, the position of the thermal front is expressed as [21]

$$r_f^2 = \frac{\rho_w c_w}{\rho_a c_a} \frac{Qt}{\pi h} \quad . \tag{1}$$

If Eq. 1 is divided by the dimensionless radial distance to the front r_{Df}^2, then the movement of the front can be expressed as

$$\frac{t}{r_{Df}^2} = \frac{\rho_a c_a}{\rho_w c_w} \frac{\pi h}{Q} r_w^2 \quad . \tag{2}$$

By evaluating Eq. 2 at the well it can be seen that the change of slope on the semi-log straight line occurs at

$$t_o \approx \frac{\rho_a c_a \pi h}{\rho_w c_w Q} r_w^2 \qquad (3)$$

For example, at an injection rate of 1 X 10^{-4} $m^3/s/m$, with an injected fluid density of 900 kg/m^3, and the reservoir properties listed in Table 1; t_o is equal to 240 s.

Numerous simulations were conducted to determine the dependence of t_o on the rock permeability, porosity, compressibility, injection temperature, reservoir temperature, and flow rate. These studies verified that Eq. 3 gives a reasonable approximation for the intersection of the two lines of different slopes. For example, Figure 3 shows the pressure transient behavior due to injecting fluids at 50°C, 100°C, and 150°C into a 250°C reservoir (see Table 1 for reservoir properties). In each case, the pressure data fall first on the "hot slope" and then on the corresponding "cold slope". Note that the time of intersection, t_o, is nearly identical for each case.

Because injection tests are often conducted after the well has been cooled by drilling, or after an extended period of injection, the effect of a "cold spot" around the injection well must also be considered. Figure 4 shows the pressure transients during 100°C water injection where pre-existing 1-m, 5-m, and 10-m cold (100°C) spots are present. The reservoir properties are the same as those used in the preceding examples (see Table 1). In essence, at early times, the reservoir acts as a composite system with an inner-region mobility of k/μ_i and an outer-region mobility of k/μ_r. In this light, the

simulated data shown in Figure 4 is easily understood. The pressure data initially follow the slope corresponding to the cold spot (mobility = k/μ_i). When the drainage radius exceeds the radius of the cold spot, a transition occurs during which the slope changes to that of the hot outer region (mobility k/μ_r). This will occur at a time given by [22]

$$t_f = \frac{\phi \mu_i \beta_t r_f^2}{4k} \quad . \tag{4}$$

For the reservoir properties listed in Table 1, the drainage radius will exceed a 10-m cold spot in 140 s, a 5-m cold spot in 35 s and a 1-m cold spot in approximately 1 seconds.

After a period of time, the pressure data again change slope (see Fig. 4) and become identical to the no-cold-spot pressure transient. The time at which second transition occurs can be approximated by

$$t'_o = \frac{\rho_a c_a}{\rho_w c_w} \frac{\pi h}{Q} r_f^2 \quad . \tag{5}$$

For a flow rate of 1×10^{-4} $m^3/s/m$ and the reservoir properties listed in Table 1, t'_o is 20 days for a 10-m cold spot, 5 days for a 5-m cold spot, and 5 hours for a 1-m cold spot.

Effect of Skin Factor

Simulation of nonisothermal injection into wells with both positive and negative skin factors has also been carried out. The skin is modeled

as an annular region of reduced or enhanced permeability around the well. The corresponding skin factors are given by[22]

$$s = \left(\frac{k}{k_s} - 1\right) \ln\left(\frac{r_s}{r_w}\right). \tag{6}$$

Figure 5 shows simulated pressure transient data at the well for several skin factors. (The reservoir properties used in these simulations are given in Table 1.) The effect of the skin factor is to displace the absolute pressure change and shift t_o by a factor of e^{-2s}. Therefore, the transition time is modified and becomes

$$t_o \cong \frac{\rho_a c_a \pi h \; r_w^2 e^{-2s}}{\rho_w c_w \; Q} . \tag{7}$$

The problem is more complex if there is a pre-existing cold spot around the well. The system is then divided into three regions: the skin region with a mobility of k_s/μ_i, the cold spot with mobility k/μ_i, and the hot reservoir with a mobility k/μ_r. In Figure 6, the pressure transients for 100°C water injection into a 250°C reservoir with a 3-m cold spot (100°C) are given for several of the skin factors. The figure shows that the skin factor only displaces the curve, without changing the slopes or transition times.

Wellbore Effects

In the preceding discussions the influence of wellbore effects have been neglected. Both the thermal transients in the wellbore and the effects of wellbore storage must be considered. If a free liquid level is present in the wellbore, storage effects will be large and may mask much of the early-time pressure data. Therefore, the first semi-log straight line may not be apparent. The analysis methods presented in this paper do not require the presence of the first semi-log straight line. It is sufficient to evaluate the duration of wellbore storage using conventional methods and to check that the semi-log straight line used for the analysis begins after storage effects have ceased.

Thermal transients may also influence the early-time pressure data. If the well is deep or the casing diameter is large, it will take a significant period of time before the bottomhole injection temperature stabilizes. The importance of this will depend primarily on the pre-injection temperature profile in the well, the injection rate, the depth of the interval being tested, and the pre-test well history. For a well that is cooled by previous injection the thermal transients are negligible. On the other hand, if the well is hot, the effect of initially injecting a column of hot fluid must be considered. Because the pre-test temperature profile and the well completion are site-specific, it is not possible to develop a simple correction for these effects. However, t_o will be delayed until the bottomhole temperature stabilizes. If thermal transients are significant, t_o, must be evaluated with a well/reservoir simulator. Careful test planning can be used to avoid the effects of thermal transients on the data. For instance, for composite reservoir behavior and falloffs, the pressure data are unaffected by thermal wellbore transients.

Discussion

The pressure transient response of nonisothermal injection with a moving thermal front has been demonstrated. Clearly, the pressure transient data can be used to calculate the reservoir transmissivity, kh/μ, from one of the semi-log straight lines on the pressure vs. log (time) plot. If the fluid properties to which the slope corresponds can be determined, then kh of the reservoir can be determined. Furthermore, if the first slope is apparent, either in the case of a cold spot or a moving thermal front, then the correct skin value can be calculated.

In practice, however, the first slope and the first break in slope may be masked by well bore storage. The second break in slope (for injection with a pre-existing cold spot) will usually not be detected during a test, because it occurs at fairly late times, even for small cold spots. Therefore, it is important to be able to determine independently the fluid properties to which the analyzed portion of the data correspond and to develop a method for calculating the skin in the absence of the first slope.

By examining Figures 2, 3, and 5, it can be seen that the pressure transient response with no cold spot is identical to that of cold isothermal injection, except for a short period during which the pressure changes correspond to the reservoir fluid properties. The pressure offset that is created between the two curves is a function of t_o, μ_r, μ_i, and the density contrast of the fluids. This offset, Δp_o, can easily be calculated if kh and $\phi\beta_t h$ are known. Since kh/μ_i can be determined from the pressure vs. log (time) graph and $\phi\beta_t h$ can be estimated from well log data, the offset between the curves can be calculated from

$$\Delta p_o = \frac{q}{2\pi kh} \left(\frac{\mu_i}{\rho_i} p_D \ (t_{Do})_i - \frac{\mu_r}{\rho_r} p_D \ (t_{Do})_r \right) \tag{8}$$

where

$$(t_{Do})_i = \frac{kt_o}{\phi \mu_i \beta_t r_w^2}, \text{ and } (t_{Do})_r = \frac{kt_o}{\phi \mu_r \beta_t r_w^2} . \tag{8a,b}$$

If the wellbore storage effects are small and the wellbore thermal transients can be neglected, t_o can be calculated by Eq. 3.

As stated before, a reservoir with a cold spot can be envisioned as a composite reservoir with an inner-region mobility of k/μ_i and an outer-region of mobility k/μ_r. If the inner region is small enough (<200 X rw), it can be treated as a pseudo-skin around the well, with a radius of r_f. The pseudo-skin, henceforth referred to as the thermal skin, can be calculated in a manner analogous to the calculation of a conventional skin (Eq. 6) except that the mobility is substituted for the permeability and is given by

$$s_t = \left(\frac{k\rho_r/\mu_r}{k\rho_i/\mu_i} - 1 \right) \ln \left(\frac{r_f}{r_w} \right) . \tag{9}$$

Since k is the same in both regions, the thermal skin is be given by

$$s_t = \left(\frac{\mu_i \rho_r}{\mu_r \rho_i} - 1 \right) \ln \left(\frac{r_f}{r_w} \right) . \tag{10}$$

The steady state pressure change associated with s_t can be calculated from

$$\Delta p_{st} = 0.87 \ m_r s_t . \tag{11}$$

In the following sections, procedures for analyzing nonisothermal injection and falloff tests are developed. The procedures are based on the above discussions and follow conventional analysis methods as closely as possible. S.I. units are used throughout the development of the methods, but in the application to a field example given in the final section, the formulas are converted to correspond to standard oil field units.

ANALYSIS OF NONISOTHERMAL INJECTION TESTS

Methods for analyzing injection data fall into two categories: that used when there has been no injection prior to the test and that used when the well has been used for injection prior to the test. The first case may occur when an injection test is being used to determine the reservoir characteristics or perhaps when injection is being carried out in an attempt to stimulate the well. An injection well being tested for diagnostic purposes will fit into the latter case. The analysis method for each case is developed separately.

Analysis of No-Cold-Spot Injection Tests

Initially, in the case of nonisothermal injection without a cold spot the pressure buildup is controlled by the in situ fluid temperature. Later the increase in slope at t_o (Eq. 3) indicates that the pressure buildup is governed by the temperature of the injected fluid. This usually happens within the first several minutes of the test and may therefore be masked by wellbore storage effects. Thus the slope corresponding to injected fluid is often the only one that will be apparent. The following procedure is used to estimate the reservoir kh and skin factor when the thermal wellbore transients are negligible. If they are significant, t_o must be evaluated using a

numerical simulator.

1) Use Eq. 3 to estimate the time at which the slope of the pressure transient changes to that of the injected fluid.

2) Estimate the duration of wellbore storage by conventional methods.

3) On a plot of pressure vs. log (time), find a straight line from which kh can be calculated (make sure that the data being analyzed are after t_o and that wellbore storage effects have ceased). Then, calculate.

$$kh = 0.183 \frac{q\mu_i}{\rho_i m_i} \quad . \tag{12}$$

4) Use Eq. 8 to calculate the pressure offset for the isothermal and nonisothermal injection.

5) Extrapolate the semilog straight line (m_i) to 1 second and determine Δp_{1s}. Calculate

$$\Delta p^*_{1s} = \Delta p_{1s} + \Delta p_o \quad . \tag{13}$$

6) Calculate the skin factor,

$$s = 1.151 \left(\frac{\Delta p^*_{1s}}{m_i} - \log \frac{k}{\phi \mu_i \beta_t r_w^2} - 0.351 \right) \quad . \tag{14}$$

7) Re-evaluate t_o using Eq. 7 to ensure that the data used to calculate the slope of the semi-log straight line corresponds to the properties of the injected fluid. Repeat the above procedure if the incorrect data were used.

The data shown in Figure 5 were analyzed using this procedure. The results are summarized in Table 2 where the skin factors, calculated skin factors and apparent skin factors are given. The effect of ignoring nonisothermal pressure transients during cold water injection (with no cold spot) is to underestimate the skin factor. In fact, even a well with a positive skin may appear to have a negative skin. The larger the viscosity contrast between the injected and in situ fluids the more the skin factor will be underestimated.

Analysis of "Composite Reservoir" Injection Tests

The pressure response to injection of cold water into a hot reservoir with a cold spot around the well can be described in terms of three periods. The first corresponds to the pressure transient associated with the cold spot of radius r_f, the second to the hot reservoir outside the cold spot, and the third to the behavior dominated by the moving front. For a sufficiently large cold spot, the first slope may be apparent; if so, it can be used to calculate kh and the skin factor.[2-6] However, the first slope is commonly masked by the effects of wellbore storage, in which case another method of analysis is needed.

To obtain a reasonably accurate analysis of the pressure transient data, it is important to have an estimate of the cummulative injection (C) into the reservoir. If this is available, then the following procedure can be used.

1) Estimate the size of the cold spot from

$$r_f \cong \sqrt{\frac{C}{\pi h}\frac{\rho_w c_w}{\rho_a c_a}} \quad . \tag{15}$$

2) Use Eq. 4 to calculate the time at which the hot slope will begin; and Eq. 5 to compute the time at which the second cold slope will begin.

3) Estimate the duration of wellbore storage by conventional methods.

4) From the slope m_r on a plot of pressure vs. log (time) calculate

$$kh = 0.183 \frac{\mu_r}{\rho_r}\frac{q}{m_r} \quad . \tag{16}$$

Make sure that the correct slope has been chosen by comparing the beginning and ending times to the values obtained in steps 2 and 3.

5) Use Eq. 10 to calculate the thermal skin factor associated with the cold spot.

6) Use Eq. 11 to calculate the pressure drop attributed to the cold spot.

7) Extrapolate m_r to obtain Δp_{1s} and calculate

$$\Delta p^*_{1s} = \Delta p_{1s} - \Delta p_{st} \quad . \tag{17}$$

8) Calculate the skin factor for the well

$$s = 1.151 \frac{\mu_r \rho_i}{\mu_i \rho_r}\left(\frac{\Delta p_{1s}}{m_r} - \log \frac{k}{\phi \mu_r \beta_t r_w^2} - 0.351\right) \quad . \tag{18}$$

Example

In this example, 100°C water is injected into a 250°C reservoir with a 3-m cold spot around the well. The cold spot is the same temperature as the injected fluid, and the injection rate is 0.1 kg/s/m. Table 1 gives

the reservoir properties used for this simulation. The well has a skin factor of +2. Figure 7 shows the pressure transient data. The data initially follow a slope that corresponds to the fluid properties of the cold spot. After 20 s, the data fall on the slope corresponding to the fluid properties of the hot reservoir. At approximately 1.5×10^5 s (~42 hours), the data again change to the cold slope. This last transition corresponds to the time at which the moving thermal front starts to dominate the pressure response. The departure from the first slope can be calculated from Eq. 4:

$$t_f = \frac{(0.2)(2.79 \times 10^{-4})(1 \times 10^{-9})}{(4)(1 \times 10^{-14})} (3)^2 = 13 \text{ s} \quad .$$

The departure from the second slope can be calculated from Eq. 5:

$$t_o' = \frac{(2.57 \times 10^6)}{(960)(4200)} \frac{(\pi)(1)}{(0.1/960)} (3)^2 = 1.7 \times 10^5 \text{ s} \quad .$$

Both of these show good agreement with the observed data. From the slope m_r on the plot of pressure vs. log (time) and from Eq. 16,

$$kh = \frac{(0.183)(1.07 \times 10^{-4})(0.1)}{(811)(2.18 \times 10^5)} = 1.1 \times 10^{-14} m^3 \quad .$$

The thermal skin factor is calculated from Eq. 10,

$$s_t = \left(\frac{(2.79 \times 10^{-4})}{(1.07 \times 10^{-4})} \frac{811}{960} - 1\right) \ln\left(\frac{3}{0.1}\right) = 4.1 \ ,$$

and Eq. 11 gives

$$\Delta p_{st} = 0.87\ (2.18 \times 10^5)\ (4.1) = 7.8 \times 10^5 \text{ Pa.}$$

Extrapolating m_r to 1 second gives

$$\Delta p_{1s} = 2.44 \times 10^6 \text{ Pa,}$$

and from Eq. 17,

$$\Delta p^*_{1s} = 1.66 \times 10^6 \text{ Pa .}$$

The skin factor is calculated from Eq. 18:

$$s = 1.151 \frac{(1.07 \times 10^{-4})}{(2.79 \times 10^{-4})} \frac{811}{960} \left[\frac{(1.4 \times 10^6)}{(2.18 \times 10^5)} - \log \frac{1 \times 10^{-14}}{(0.2)(1.07 \times 10^{-4})(1 \times 10^{-9})(0.1)^2} - 0.351 \right] = 2.1 ,$$

which is in good agreement with the input data, s = 2.

If the nonisothermal effects are neglected, an apparent skin value of +10.3 is calculated by conventional methods. The input skin values, nonisothermally calculated skin values, and the apparent skin values for the pressure transient data in Figure 6 are summarized in Table 3. For cold water injection into a hot reservoir with a cold spot, a failure to account for nonisothermal behavior results in a very large overestimation of the skin factor.

PRESSURE FALLOFF BEHAVIOR AFTER NONISOTHERMAL INJECTION

After shut-in, immediately following nonisothermal injection, the reservoir behaves like a composite system with an inner region of mobility

k/μ_i, a transition region with mobility ranging from k/μ_i to k/μ_r, and an outer region of mobility k/μ_r. In this case the effects of the diffuse thermal transition were investigated. It was found that for all practical purposes, the system could be treated in terms of a two-fluid composite system. That is, the pressure transient response of a system with a diffuse thermal front is practically identical to that of one with a sharp front. During the pressure falloff, the thermal front moves away from the well at a negligible rate. Therefore, all of the pressure transients can be understood in terms of this composite system. There are two slopes in the falloff data, the first corresponding to the inner region and, eventually, a second slope corresponding to the in situ reservoir fluids. This is demonstrated in Figure 8, which shows a plot of falloff data after 10^5 s of cold water (100°C) injection (100°C) at a rate of 0.1 kg/s/m. The reservoir properties for this simulation are given in Table 1, except that the porosity is 0.1 and the fluid density was held constant at 1000 kg/m^3. On the plot of pressure vs. log $[(t + \Delta t)/\Delta t]$, the first slope, m_i, is apparent immediately after shut-in. Once the radius of investigation is greater than the size of the cold spot created by 10^5 s of injection, the slope changes to that of the hot reservoir. The second slope extrapolates to the correct reservoir pressure (zero in this case because Δp is plotted). If the first break in slope is apparent, the size of the cold spot can be calculated.[2-6] Conversely, if the size of the cold spot is known (e.g. using Eq. 15), the time at which the break in slope will occur can be calculated.

The analysis of falloff data is analogous to that of injection data with an existing cold spot. Most likely, the first slope will be masked by

wellbore storage effects, so that a procedure similar to that discussed in the previous section will be required, that is,

1) Estimate r_f from Eq. 15.

2) Calculate Δt_f from Eq. 4.

3) Calculate the duration of wellbore storage (afterflow) effects using conventional methods.

4) Plot pressure vs. log $[(t + \Delta t/\Delta t]$, to obtain the slope from which kh can be calculated by means of Eq. 16. Make sure that data before Δt_f are not used for the analysis. Also make sure that the data analyzed are not affected by wellbore storage.

5) Calculate s_t from Eq. 10 and Δp_{st} from Eq. 11.

6) Extrapolate m_r to 1 second to determine p_{1s}.

   Calculate the corrected flowing pressure

$$p^*_{1s} = p_{1s} + \Delta p_{st} \quad . \tag{19}$$

7) Calculate the skin factor

$$s = 1.151 \quad \frac{\mu_r}{\mu_i}\frac{\rho_i}{\rho_r} \quad \left(\frac{(p^*_{1s} - p_{wf})}{m_r} - \log \frac{k}{\phi \mu_r \beta_t r_w^2} - 0.351\right) \quad . \tag{20}$$

Example

In this example, a pressure falloff data after 10^5 s (~1 day) of injection are analyzed (see Figure 8). The reservoir properties used in this example are given in Table 1, except that in this case the porosity is 0.1. The reservoir temperature is 250°C and the injected fluid temperature is 100°C. For this example the fluid density is held constant at 1000 kg/m^3.

After 10^5 s of injection at 0.1 kg/s/m, the thermal front has advanced 2.3 m into the reservoir (from Eq. 15). Therefore, the first slope, m_i, will end 4 s after shut-in (from Eq. 4). The second slope on the pressure vs. log [$t + \Delta t/\Delta t$] plot, m_r, can be used to calculate $kh = 9.8 \times 10^{-15}$ (from Eq. 16). The thermal skin effect is calculated from Eq. 10, $s_t = 5.0$, and the pressure buildup created by a thermal skin of 5.0 is 7.56×10^5 Pa. Extrapolating m_r to 1 second gives

$$p_{1s} = 1.05 \times 10^6 \text{ Pa},$$

from Eq. 19

$$p^*_{1s} = 1.05 \times 10^6 + 7.56 \times 10^5 = 1.8 \times 10^6 \text{ Pa} .$$

The skin factor is calculated from Eq. 20:

$$s = 1.151 \quad \frac{(1.07 \times 10^{-4})}{(2.79 \times 10^{-4})} \; \frac{(1000)}{(1000)} \left(\frac{(2.26 \times 10^6 - 1.8 \times 10^6)}{2 \times 10^5} \right.$$

$$\left. - \log \left(\frac{1 \times 10^{-14}}{(0.1)(1.07 \times 10^{-4})(1 \times 10^{-9})(0.1)^2} \right) - 0.351 \right) = 0.0 \quad .$$

This is in agreement with the input value of s = 0. If the skin value is calculated using conventional isothermal methods, a value of s = 4.4 is obtained.

A very important consequence of the apparent positive skin is that it will continue to grow with repeated injection testing or injection. This results from the growing cold spot which will appear an increasing thermal skin, s_t. For example, Table 4 summarizes the apparent skin factors for

falloff tests after 10^4, 10^5, and 10^6 s of injection at an injection rate of 0.1 kg/s/m (for the reservoir properties used in the previous example). The correctly calculated skin values are also included in the table for comparision.

FIELD EXAMPLE*

The following test data were obtained from an injection well at the East Mesa geothermal field in California.[23] Cold fluid (~50°C) was injected into well 5-1 for four days, during which downhole pressures were measured with a silicon-oil-filled capillary tubing. The test consisted of several step rates. The test segment discussed here comes from a buildup midway through the test. Table 5 summarizes the well test data.

Knowing the cumulative volume of water injected prior to the test segment to be analyzed, the thickness of the reservoir, and the thermal properties of the reservoir rock; the penetration of the thermal front into the formation can be estimated from

$$r_f = 2.37\sqrt{\frac{\rho_w c_w C}{\rho_a c_a \pi h}} \quad . \tag{21}$$

Thus, r_f = 12.5 feet for a cumulation injection of 2.3×10^4 BBL of fluid. Wellbore storage effects are small because the well is completely filled with liquid water. However, the method used to measure the downhole pressure has a response time of ~20 min for transmitting large pressure changes.[23] The drainage radius will exceed the size of the cold spot when

$$t_f = 1189.0 \frac{\phi \mu \beta_i t}{k} r_f^2 \tag{22}$$

* The equations in this section have been modified for use with oil field units.

For a 12.5-ft cold spot (k is estimated at 10 md), this will occur at approximately 50 seconds. The second change in slope, from hot to cold, will occur at

$$t_o' = 4.28 \frac{\rho_a c_a}{\rho_w c_w} \frac{\pi h}{Q} r_f^2 \tag{23}$$

approximately 43 hours after the start of this test segment. Therefore, all of the pressure data between 50 seconds and 43 hours will correspond to the fluid properties of the in situ reservoir fluids.

Figure 10 is a plot of the downhole pressure vs. log (time). The semi-log straight line begins at approximately 20 minutes. The permeability-thickness can be calculated from

$$kh = 162.6 \frac{QB_w \mu_r}{m_r} = 8400 \text{ md-ft.} \tag{24}$$

The 12.5-ft cold spot will create a thermal skin that is calculated from Eq. 10:

$$s_t = \left(\frac{0.55}{0.18} \frac{57.4}{61.8} - 1\right) \ln \left(\frac{12.5}{0.32}\right) = 6.7 \quad .$$

Δp_{st} can be calculated from Eq. 11:

$$\Delta p_{st} = 0.87 \ (48.) \ (6.7) = 281 \text{ psi} \ .$$

From the straight line on the pressure vs. log (time) plot,

$$p_{1hr} = 560 \text{ psi;}$$

and from Eq. 17,

$$p^*_{1hr} = 560 - 281 = 279 \text{ psi} .$$

The skin value is calculated

$$s = 1.151 \frac{\mu_r \rho_i}{\mu_i \rho_r} \left[\frac{p^*_{1hr} - p_i}{m_r} - \log \frac{k}{\phi \mu_r \beta_t r_w^2} + 3.2275 \right] = -1.1 \qquad (25)$$

In a previous analysis, which ignored the nonisothermal behavior, a skin value of +3.7 was calculated.[23] The positive skin value was contrary to the evidence, which suggested that the well had been inadvertently hydraulically fractured at an earlier date. The small negative skin value calculated here suggests that a fracture intersects the well. This is consistent with the well history.

CONCLUSIONS

A numerical simulator was used to study pressure transient behavior when fluid at one temperature is injected into a reservoir at another temperature. The following results have been obtained.

1) When the pressure transient behavior is controlled by a moving thermal front, the downhole properties of the injected fluid must be used to calculate kh of the reservoir.

2) If there is a pre-existing thermal discontinuity, created by previous injection, the moving thermal front will not control the pressure transient behavior until fairly late times. For most practical times, the system may be treated as a composite reservoir with an inner region of mobility k/μ_i and an outer region of mobility k/μ_r.

3) Pressure falloff data can be analyzed assuming a composite reservoir model, the inner region having a mobility of k/μ_i and the outer region having a mobility of k/μ_r. If the radius to the front is small enough the inner region can be treated as a thermal skin effect.

4) Changes in the slope of the semi-log straight line of the pressure vs. log (time) data due to non-isothermal effects may be incorrectly interpreted as reservoir boundaries.

5) If nonisothermal pressure transients are ignored, the skin value can be grossly overestimated (in the case of cold water injection into a hot reservoir with a cold spot) or underestimated (in the case of cold water injection into a hot reservoir with no cold spot).

6) Correct skin values can be calculated for nonisothermal well tests if p_{1hr} (or p_{1s}) is corrected to account for nonisothermal pressure transients.

The results of this study are quite general and are applicable to many problems in which the front moves at a rate that is proportional to t/r_f^2 and when the fluid compressibility is nearly identical on both sides of the front. Moreover, the proposed method of determining the skin value, in the absence of the first slope, may be applicable to many two-fluid composite reservoirs.

ACKNOWLEDGEMENTS

Critical review of this work by C. Goranson of the Berkeley Group Inc., and M.J. Lippmann of the Lawrence Berkeley Laboratory is appreciated.

This work was supported by the Assistant Secretary for Conservation and Renewable Energy, Office of Renewable Technology, Division of Geothermal Energy and Hydropower Technologies of the U.S. Department of Energy under Contract No. DE-AC03-76SF00098.

NOMENCLATURE

B_w = water formation volume factor, RB/STB

c = heat capacity (J/kg°C) BTU/(1b°F)

C = cumulative injection (m^3), BBL

h = reservoir thickness (m), ft

k = reservoir permeability (m^2), md

m = slope of linear portion of semilog plot of pressure transient data (Pa/cy), psi/cy

p = pressure (Pa), psi

Δp_o = pressure curve offset for nonisothermal injection with a moving front (Pa), psi

p_D = dimensionless pressure

Δp_{st} = Steady state pressure drop attributed to the region inside the front (Pa), psi

p_{wf} = pressure prior to well shut-in (Pa), psi

p_{1s} = extrapolated pressure at 1 s on a pressure vs. log (time) plot (Pa), psi

p_{1s}^* = corrected pressure on the extrapolated semilog straight line, (Pa), psi

q = mass flow rate (kg/s), 1bm/D

Q = volumetric flow rate (m^3/s), STB/D

r = radius to an observation point (m), ft

r_f = radial distance to the "thermal" front (m), ft

r_D = dimensionless radius, r/r_w

r_{Df} = dimensionless distance to the thermal front

r_w = well radius (m), ft

s = skin factor

s_t = thermal skin factor

t = time (s), hr

t_{Do} = dimensionless value of t_o

t_o = intersection time of the inner region and reservoir slopes for injection into a hot reservoir with no cold spot (s) hr

t_o' = intersection time for the change from the hot slope to the cold slope for injection with an existing cold spot (s), hr

t_f = time when the drainage radius exceeds the size of the cold spot (s), hr

t_D = dimensionless time

Greek Letters

β_t = total system compressibility (Pa^{-1}), psi^{-1}

Δ = difference

λ = thermal conductivity ($J/ms^{\circ}C$), BTU/(h ft°F)

μ = viscosity (Pa·s), cp

ϕ = porosity

ρ = density (kg/m^3), lbm/ft^3

Subscripts

a = reservoir

f = front

i = injected fluid

r = undisturbed reservoir fluid

w = water

REFERENCES

1. Hazebroek, P., Rainbow, H., and Matthews, C.S., 1958, Pressure fall-off in water injection wells: Trans. AIME, v. 213, p 250-260.

2. Larkin, K.B., 1963, Solutions to the diffusion equation for a region bounded by a circular discontinuity: Society of Petroleum Engineers Journal (June, 1963) p.113-115.

3. van Poolen, H.K., 1965, Transient tests find fire front in an in-situ combustion project: Oil and Gas Journal, p. 78-80.

4. Kazemi, H., 1966, Locating a burning front by pressure transient measurements: Journal of Petroleum Technology (February, 1966), p. 227-232.

5. Odeh, A.S., 1969, Flow test analysis for a well with radial discontinuity: Journal of Petroleum Technology (February, 1969), p.207-210.

6. Ramey, H. J , 1970, Approximate solutions for unsteady liquid flow in a composite reservoir: Journal of Canadian Petroleum technology (March, 1970), p.32-37.

7. Bixel, H.C. and van Poollen, H.K., 1967, Pressure drawdown and buildup in the presence of radial discontinuities: Soc. Pet. Eng. J., p. 301-309; Trans. AIME, v. 240. Also Reprint Series, No. 9 - Pressure Analysis Methods, Society of Petroleum Engineers of AIME, Dallas, p. 188-196.

8. Kazemi, H., Merrill, L.S., and Jargon, J.R., 1972, Problems in interpretation of pressure fall-off tests in reservoirs with and without fluid banks: Journal of Petroleum Technology, p. 1147-1156.

9. Merrill, L.S., Jr., Kazemi, H., and Gogarty, W.B., 1974, Pressure falloff analysis in reservoir with fluid banks: Journal of Petroleum Technology (July 1984), p. 809-818.

10. Satman, A., Eggenschwiller, M., Tang, R.W., and Ramey, H.J., Jr., 1980, An analytical study of transient flow in systems with radial discontinuities: SPE-9399, presented at the 55th Annual Meeting of the Society of Petroleum Engineers, September 21-24, 1980.

11. Bodvarsson, G.S. and Tsang, C.F., 1980, Thermal effects in the analysis of fractured reservoirs, in 3rd Invitational Well Testing Symposium: Lawrence Berkeley Laboratory Report LBL-12076, Berkeley, California, p. 110-119.

12. Tsang, Y.W. and Tsang, C.F., 1978, An analytic study of geothermal reservoir pressure response to cold water reinjection: in Proceedings, 4th Workshop on Geothermal Reservoir Engineering, Stanford University, Stanford, California, December 13-15, SGP-TR-30, p. 322-331.

13. O'Sullivan, M.J. and Pruess, K., 1980, Analysis of injection testing of geothermal reservoirs: Geothermal Resources Council, v. 4, p. 401-404.

14. Garg, S.K., and Pritchett, J.W., 1981, Cold water injection into two-phase geothermal reservoirs: in Proceedings of the 7th Workshop of Geothermal Reservoir Engineering, Stanford University, Stanford, California, December 15-17, 1981, SGP-TR-55, p. 175-178.

15. Bodvarsson, G.S., Benson, S.M., Sigurdsson, O., Halldorsson, G.K., and Stefansson, V., 1981, Analysis of well data from the Krafla Geothermal field in Iceland: Proceedings of the Seventh Workshop on Geothermal Reservoir Engineering, Stanford University, Stanford, California, December 15-17, SGP-TR-55, p. 71-76.

16. Gobran, B.D., Brigham, W.E., and Sanyal, S.K., 1980, The temperature dependence of permeability: Geothermal Resources Council, TRANSACTIONS v. 4, p. 397-400.

17. Edwards, A.L., 1972, TRUMP: A computer program for transient and steady-state temperature distribution in multidimensional systems: Lawrence Livermore Laboratory Report UCRL-14754, Rev. 4.

18. Duff, I.S., 1977, MA28 - A set of Fortran subroutines for sparse unsymmetric linear equations: Harwell Report AERE-R 8730, Oxfordshire, Great Britain.

19. Doughty, C., Buscheck, T.A., and Tsang, C.F., (1983), Prediction and analysis of a field experiment on a multi-layered aquifer thermal energy storage system with strong bouyancy flow: Water Resources Research (October, 1983), Vol.19, No.5, p.1307 - 1315.

20. Bodvarsson, G.S., 1981, Mathematical modeling of the behavior of geothermal systems under exploitation: Ph.D. dissertation, University of California, Berkeley, Ca.

21. Bodvarsson, G., 1969, On the temperature of water flowing through fractures: Journal of Geophysical Research, v. 74, no. 8, p.1987-1992

22. Earlougher, R.C., Jr., 1977, Advances in well test analysis: Society of Petroleum Engineers, Monograph.

23. McEdwards, D.G. and Benson, S.M., 1978, Results of two injection tests at the East Mesa KGRA: in Second Invitational Well-Testing Symposium, Lawrence Berkeley Laboratory Report LBL-8883, p.34-40.

Table 1. Reservoir parameters used in the simulation.

k	1.0×10^{14} m^2
h	1.0 m
ϕ	0.2
$\rho_a c_a$	2.57×10^6 $J/m^3{}^\circ C$
λ	0.1 $J/m^\circ C$ s
r_w	0.1 m
β_t	1×10^{-9} Pa^{-1}
T_r	250°C

Table 2. Skin factor analysis for pressure transient data shown in Figure 5.

Input Skin	Calculated Skin (nonisothermal)	Apparent* Skin
5.7	5.6	3.0
3.6	3.6	0.9
1.6	1.6	-1.1
0.0	0.1	-2.7
-2.3	-2.3	-4.9

*Apparent skin factors are calculated using standard isothermal analysis methods. (See reference 22).

Table 3. Comparison between input and calculated skin values for the pressure transient data in Figure 6.

Input Skin	Calculated Skin (nonisothermal)	Apparent Skin
5.0	5.0	18.3
2.0	2.1	10.3
0.0	-0.2	3.6
-2.0	-2.0	0.2

Table 4. Skin factor analysis after 10^4, 10^5, and 10^6 s of 100°C injection into a 250°C reservoir.

Cumulative Injection (kg)	r_f (m)	Input Skin	Calculated Skin (nonisothermal)	Apparent Skin
1×10^3	0.7	0.0	-0.2	2.5
1×10^4	2.2	0.0	-0.2	4.4
1×10^5	7.	0.0	0.0	6.0

Table 5. Well and test data for well 5-1 at East Mesa.

Well radius	0.32 ft
Well depth	6000 ft
Open interval	4000-6000 ft
Injection interval (h)	4000-4400 ft
Reservoir temperature	150°C
Injection temperature (sandface)	50°C
Rock type	Sandstone
Porosity (φ)	0.2
Total compressibility (β_t)	7.0×10^{-6} psi^{-1}
B_w	1.08 RB/STB
Flow rate (Q) - surface rate	1.27×10^4 STB/D
Static pressure (P_i)	135 psi*
Cumulative injection	2.3×10^4 BBL

*This is only a relative value because downhole pressures were measured with an oil-filled capillary tube.

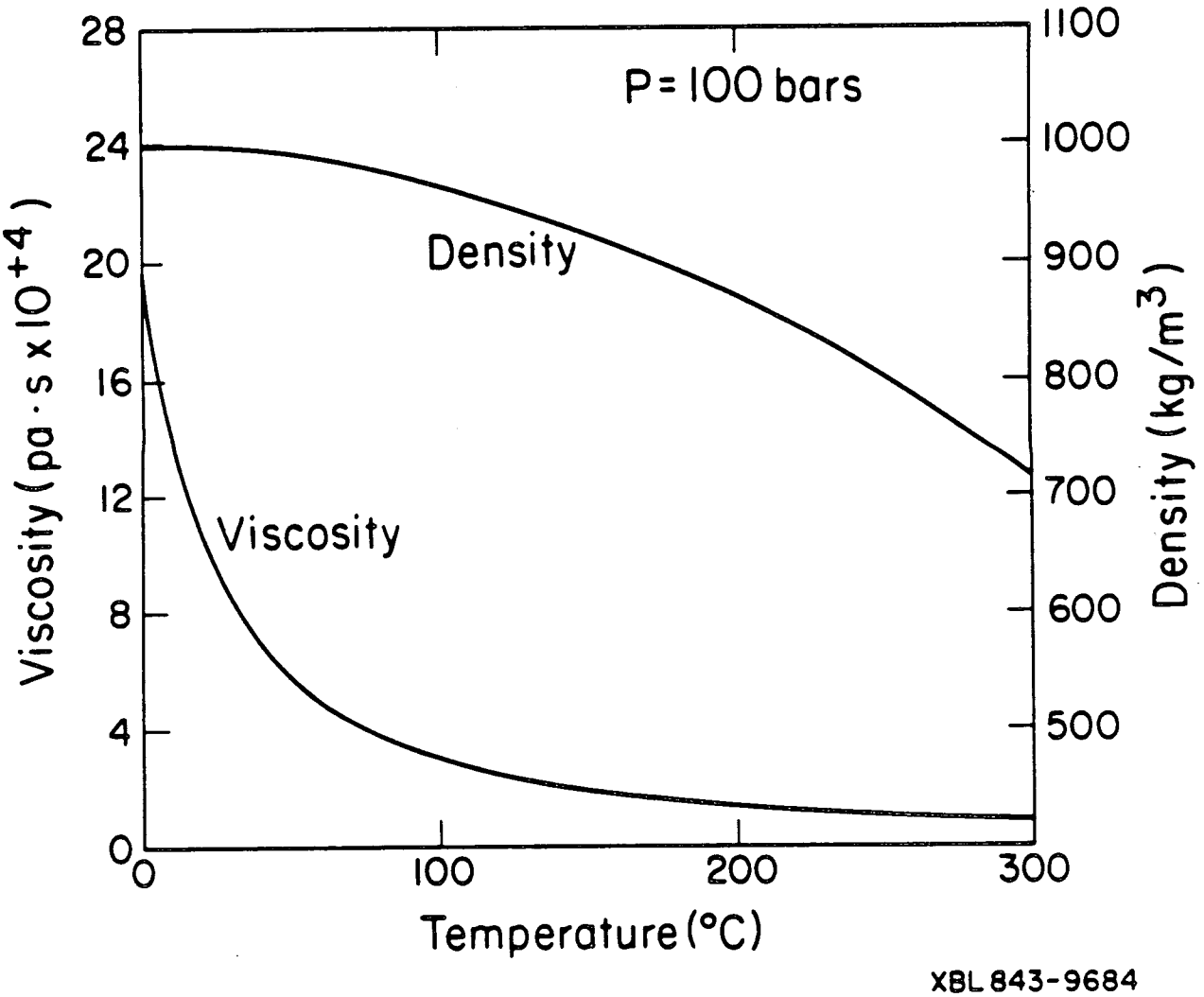

Figure 1. Dynamic viscosity and density of water between 0°C and 300°C at a pressure of 100 bars.

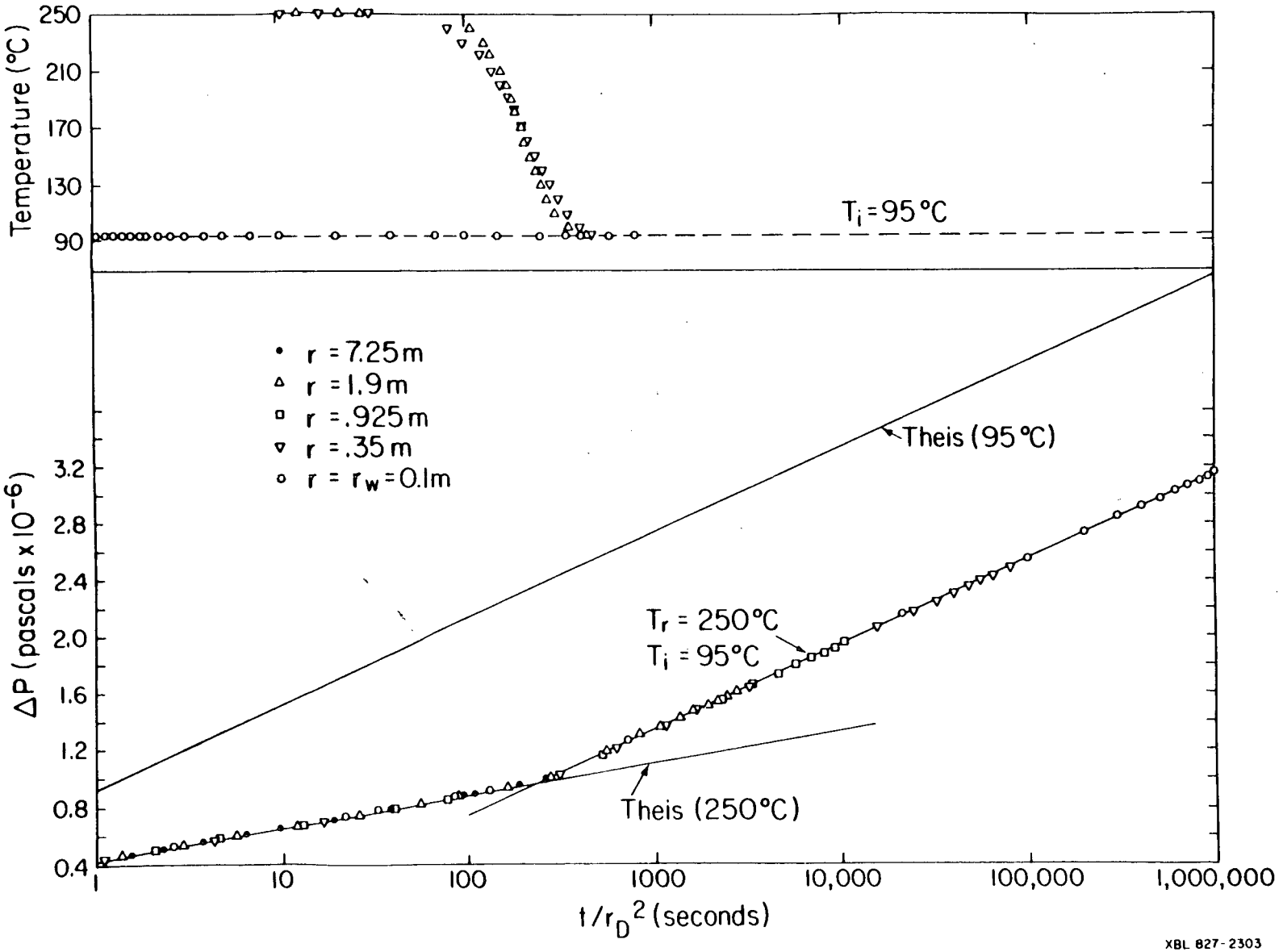

Figure 2. Pressure transient data for injection of 95°C water into a 250°C reservoir.

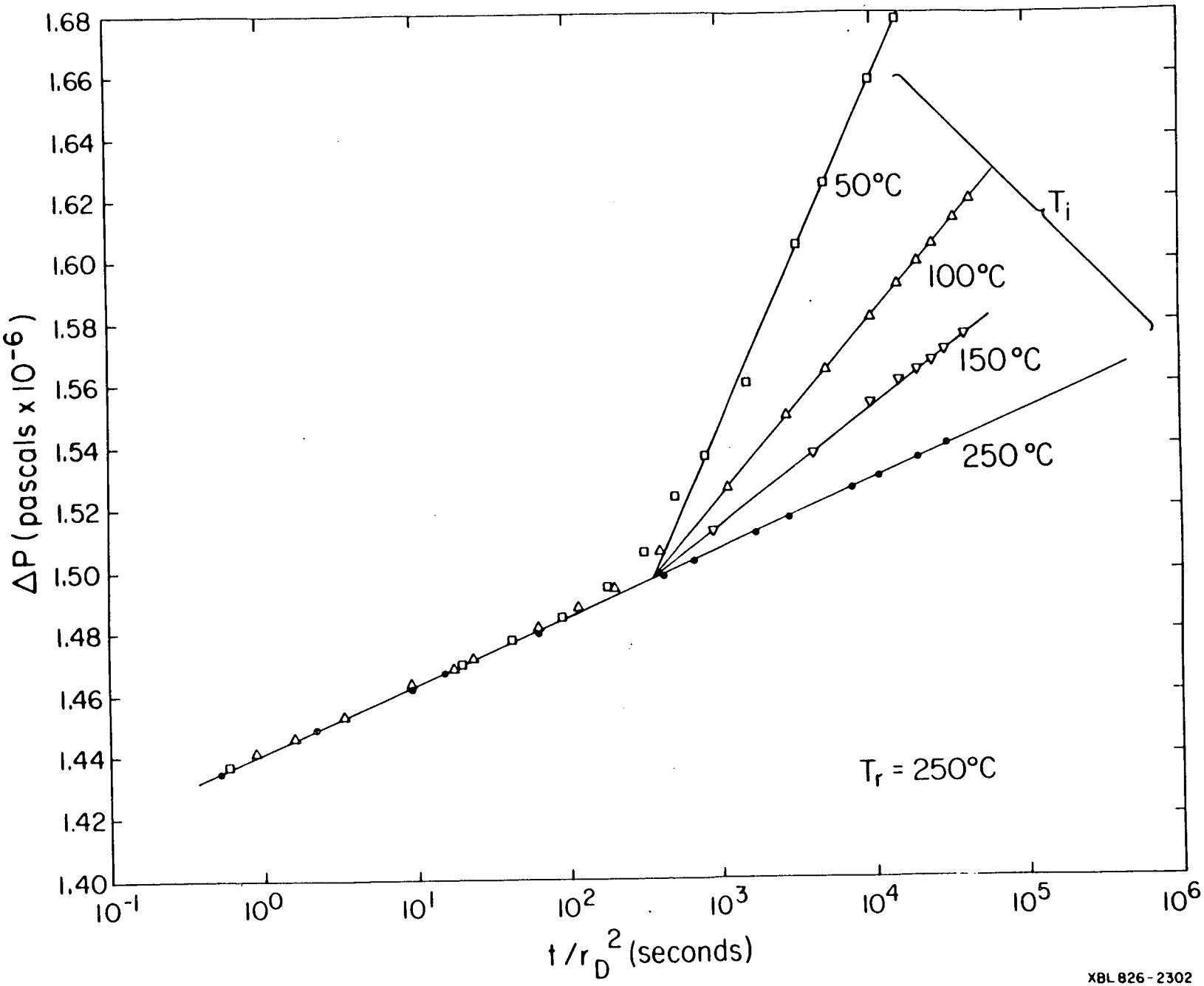

Figure 3. Pressure transient data for injection of 50°C, 100°C, and 150°C water into a 250°C reservoir.

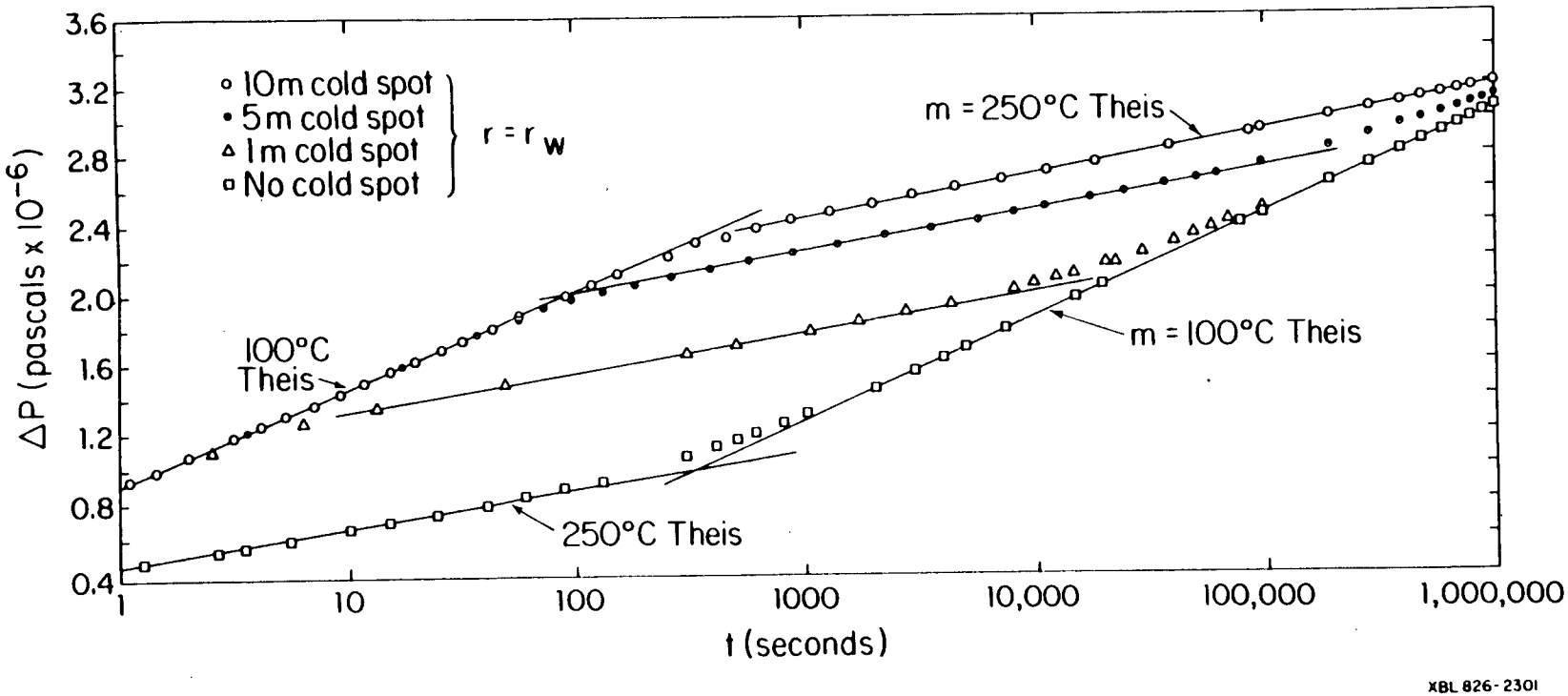

Figure 4 Pressure transient data for injection of 100°C water into a 250°C reservoir with cold spots around the well.

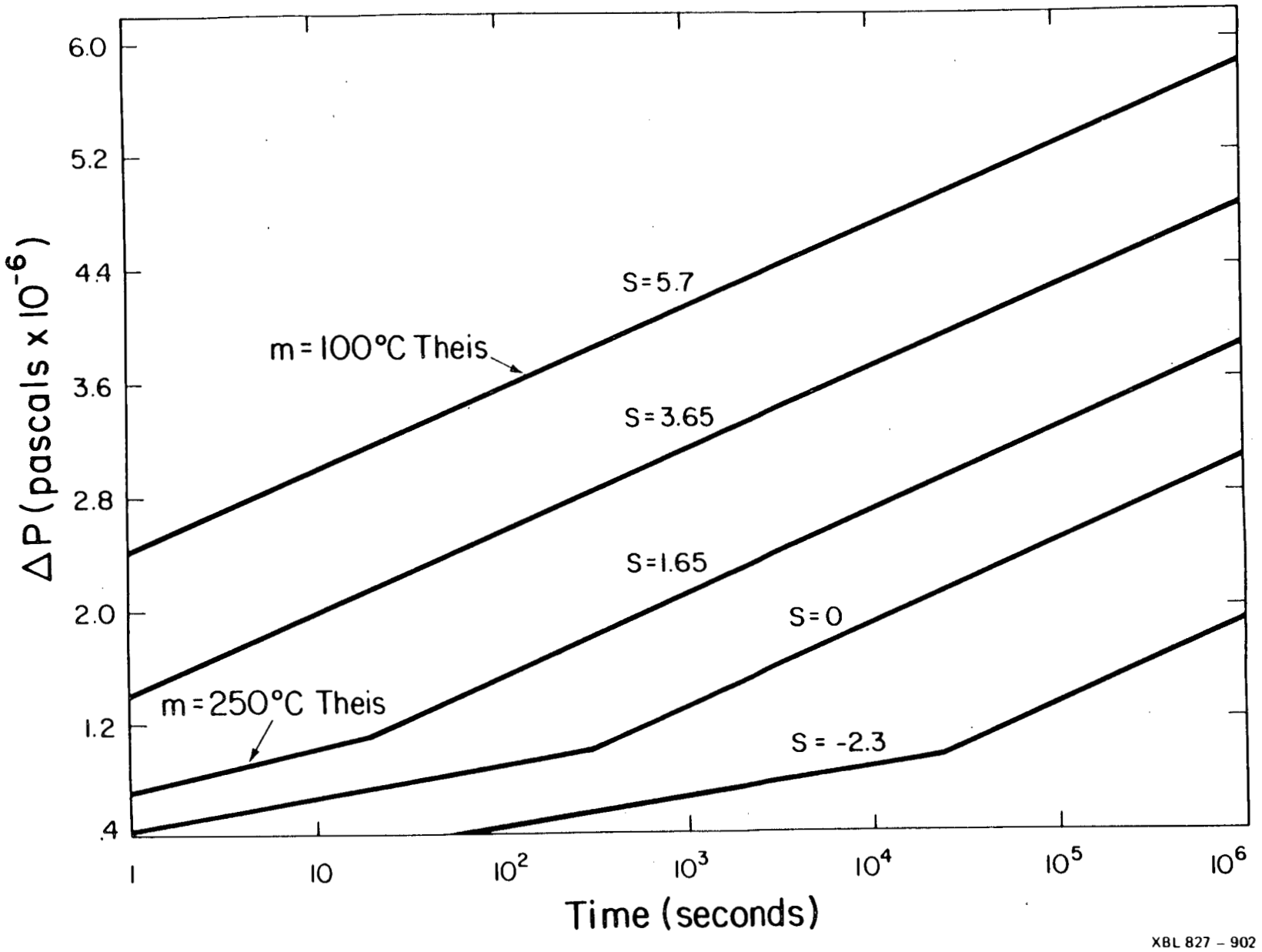

Figure 5. Pressure transient data for 100°C injection into a 250°C water reservoir for a well with several different skin values.

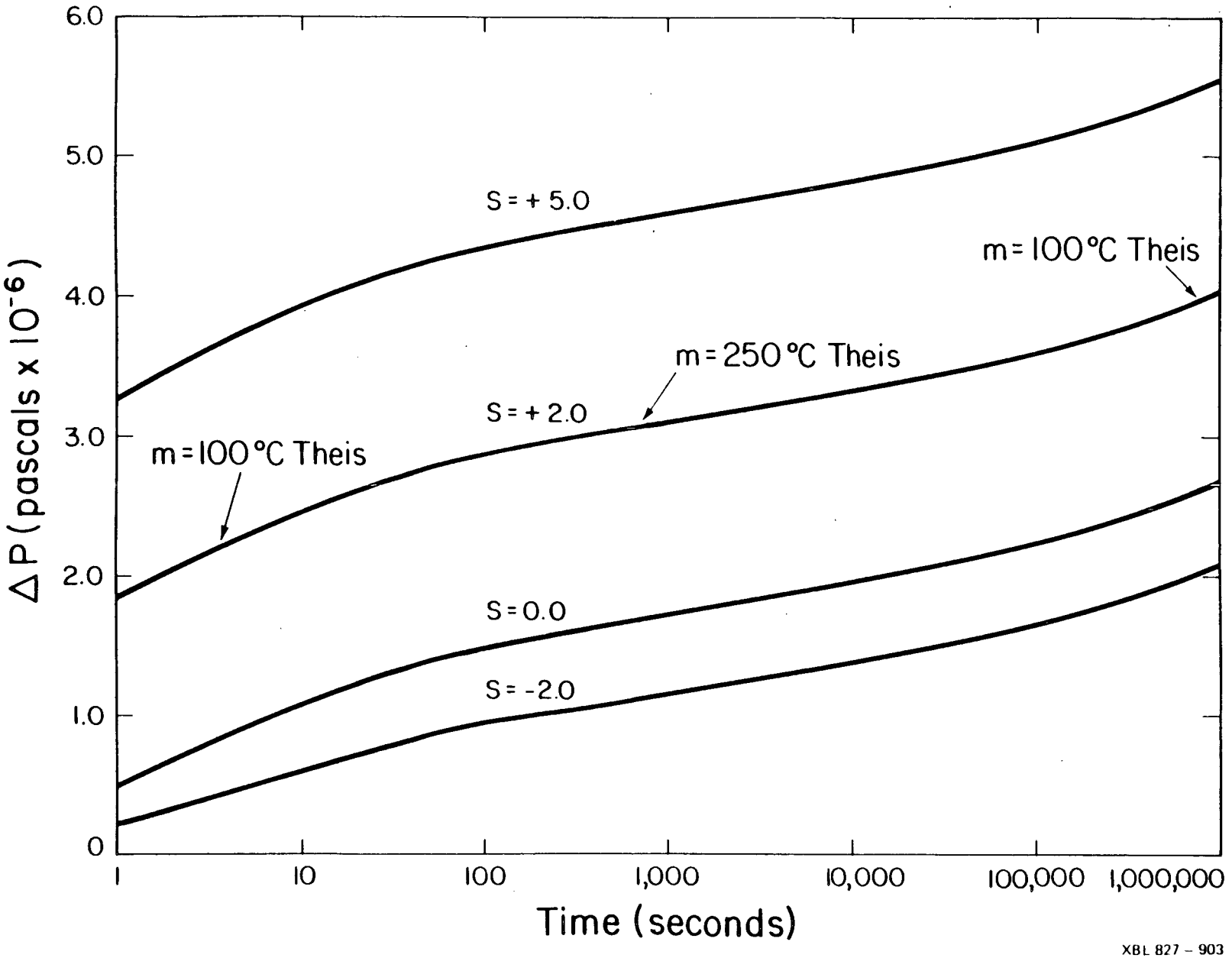

Figure 6. Pressure transient data for 100°C injection into a 250°C reservoir with a 3-m cold spot and several skin values.

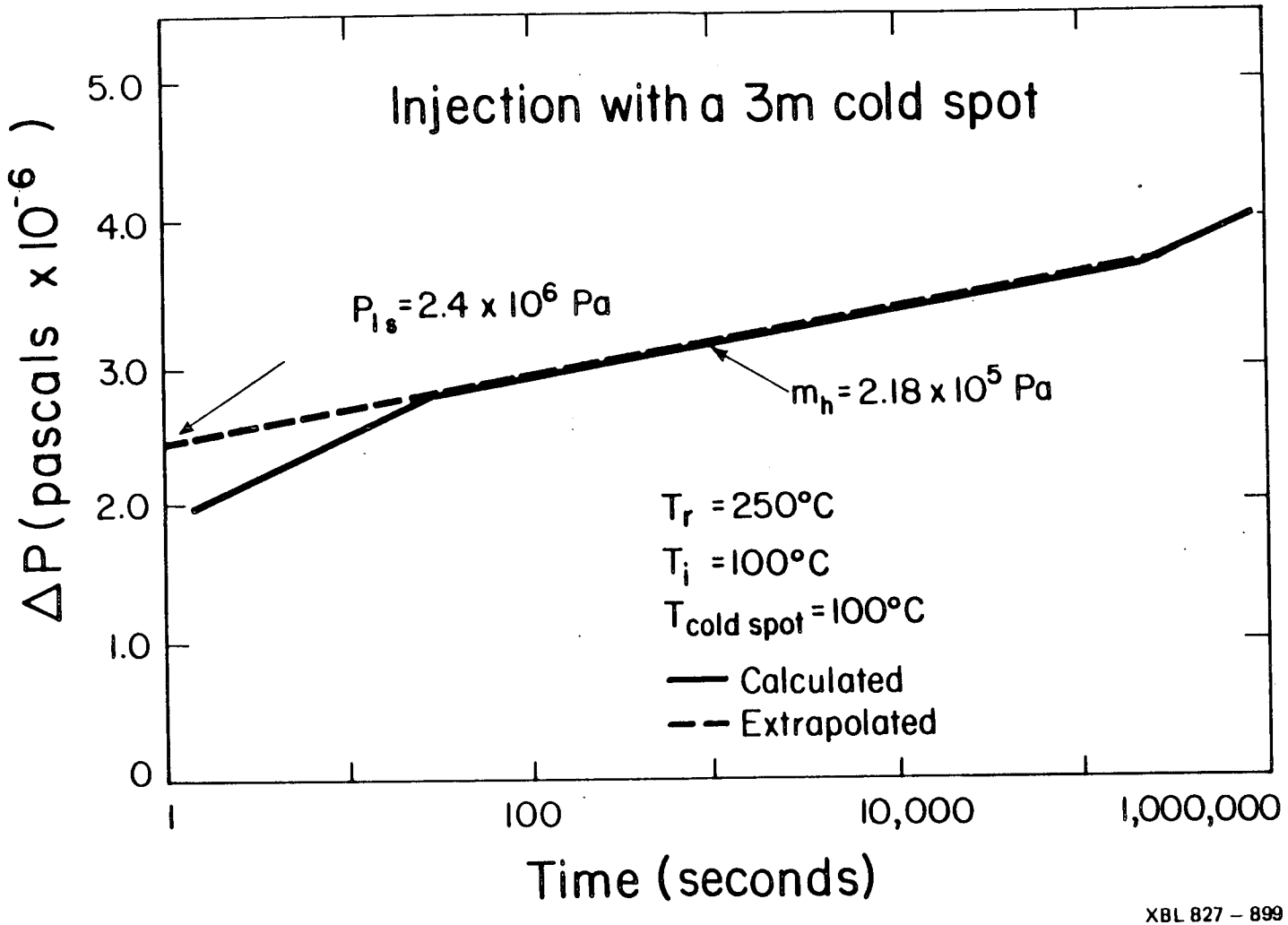

Figure 7. Pressure buildup data for Example 1: Injection test analysis for a well surrounded by a 3-m cold spot.

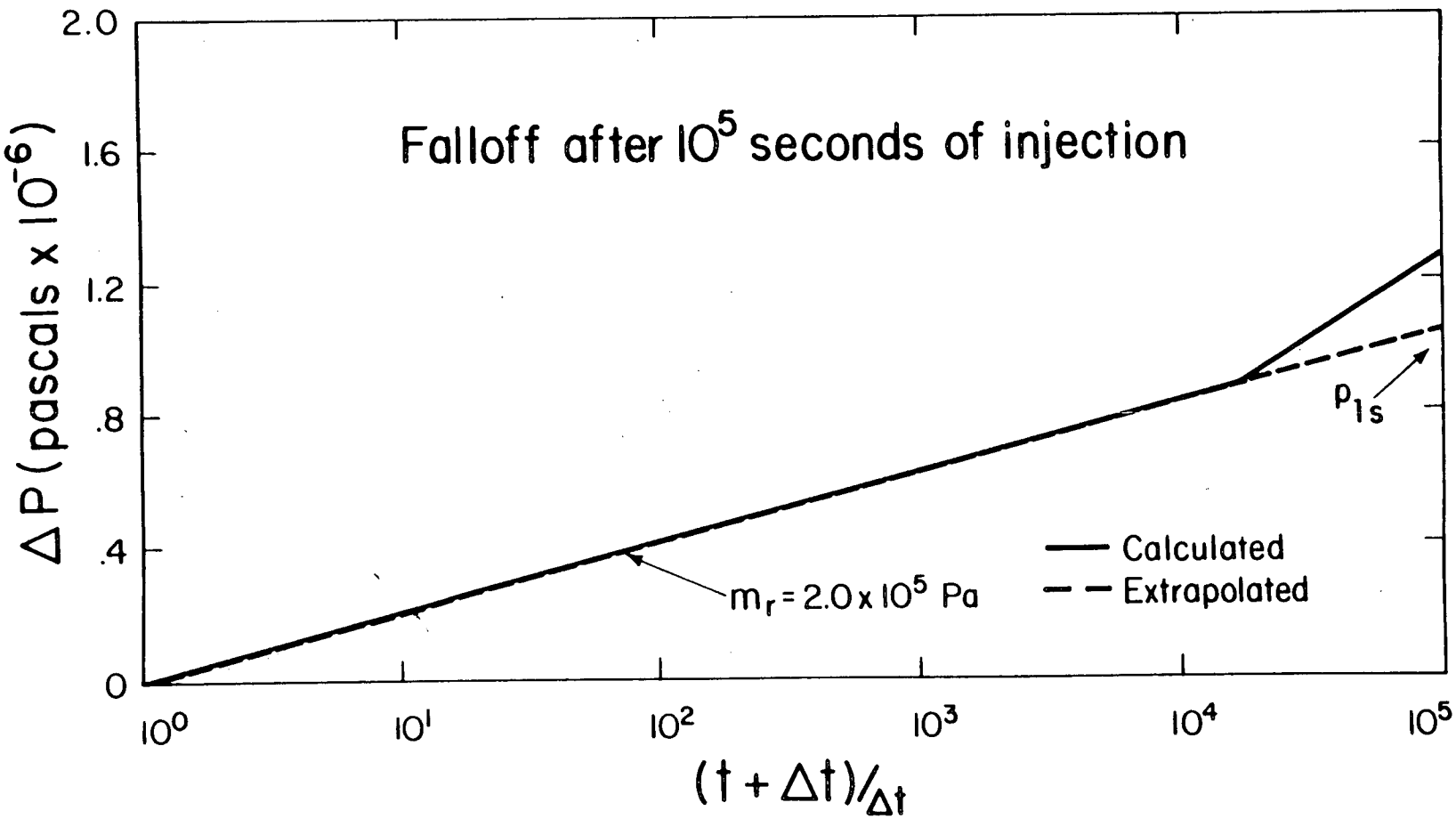

XBL 827 – 896

Figure 8. Pressure falloff data for Example 2: Falloff analysis after 10^5 seconds of 100°C injection into a 250°C reservoir.

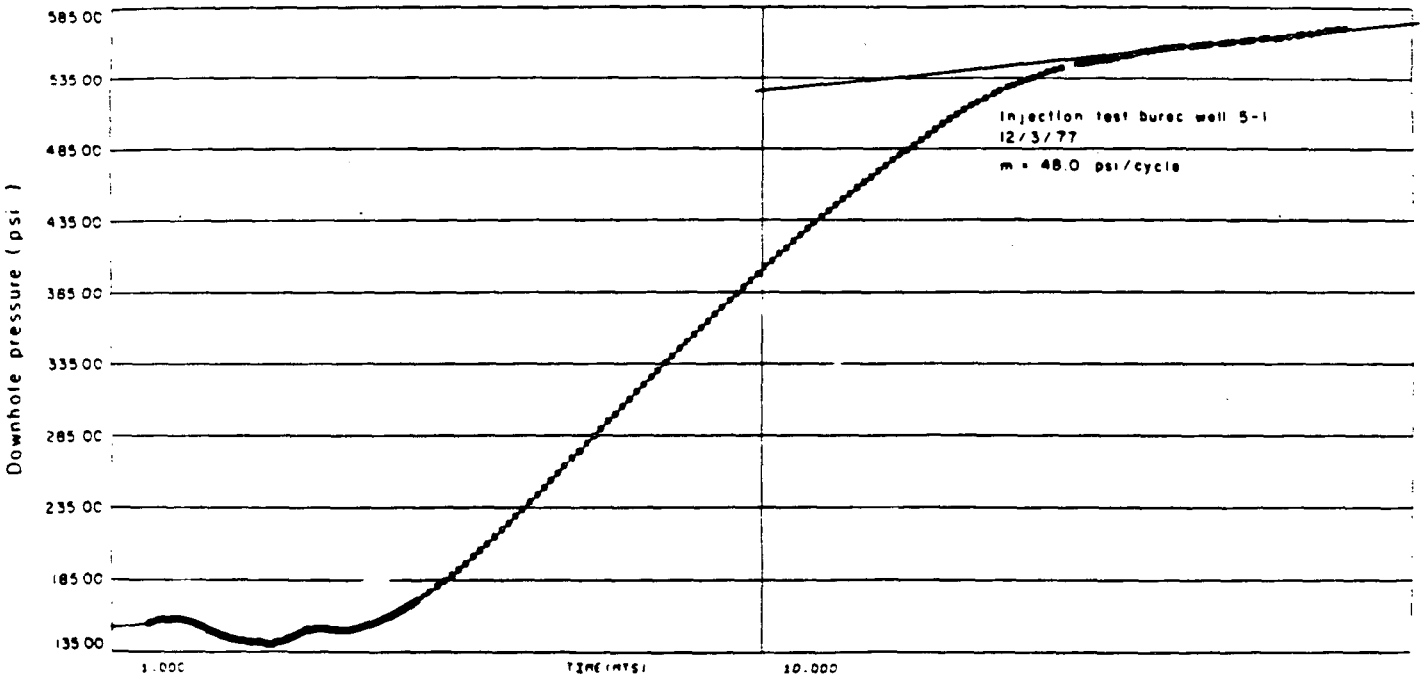

Figure 9. Pressure buildup data from well 5-1 at the East Mesa Geothermal Field, California.

This report was done with support from the Department of Energy. Any conclusions or opinions expressed in this report represent solely those of the author(s) and not necessarily those of The Regents of the University of California, the Lawrence Berkeley Laboratory or the Department of Energy.

Reference to a company or product name does not imply approval or recommendation of the product by the University of California or the U.S. Department of Energy to the exclusion of others that may be suitable.